J Mater Sci: Mater Med (2011) 22:405–416
DOI 10.1007/s10856-010-4193-3

Immobilization and bioactivity evaluation of FGF-1 and FGF-2 on powdered silicon-doped hydroxyapatite and their scaffolds for bone tissue engineering

María José Feito · Rosa María Lozano · María Alcaide · Cecilia Ramírez-Santillán · Daniel Arcos · María Vallet-Regí · María-Teresa Portolés

Received: 22 July 2010 / Accepted: 19 November 2010 / Published online: 4 December 2010

Abstract Fibroblast growth factors (FGFs) are polypeptides that control the proliferation and differentiation of various cell types including osteoblasts. FGFs are also strong inducers of angiogenesis, necessary to obtain oxygen and nutrients during tissue repair. With the aim to incorporate these desirable FGF biological properties into bioceramics for bone repair, silicon substituted hydroxyapatites (Si-HA) were used as materials to immobilize bioactive FGF-1 and FGF-2. Thus, the binding of these growth factors to powdered Si-HA and Si-HA scaffolds was carried out efficiently in the present study and both FGFs maintained its biological activity on osteoblasts after its immobilization. The improvement of cell adhesion and proliferation onto Si-HA scaffolds suggests the potential utility of these FGF/scaffolds for bone tissue engineering.

Keywords Fibroblast growth factor · Hydroxyapatite · Scaffold · Bone tissue engineering · Osteoblast

M. J. Feito · M. Alcaide · C. Ramírez-Santillán · M.-T. Portolés (✉)
Department of Biochemistry and Molecular Biology I, Faculty of Chemistry, Universidad Complutense, 28040 Madrid, Spain
e-mail: portoles@quim.ucm.es

M. J. Feito
e-mail: mjfeito@bbm1.ucm.es

M. Alcaide
e-mail: marialcaide_2000@yahoo.es

C. Ramírez-Santillán
e-mail: cecilia27884@hotmail.com

R. M. Lozano
Department of Physical and Chemical Biology, Centro de Investigaciones Biológicas, Consejo Superior de Investigaciones Científicas, 28040 Madrid, Spain
e-mail: rlozano@cib.csic.es

D. Arcos · M. Vallet-Regí
Department of Inorganic and Bioinorganic Chemistry, Faculty of Pharmacy, Universidad Complutense, 28040 Madrid, Spain
e-mail: arcosd@farm.ucm.es

M. Vallet-Regí
e-mail: vallet@farm.ucm.es

D. Arcos · M. Vallet-Regí
Networking Research Center on Bioengineering, Biomaterials and Nanomedicine, Madrid, Spain

1 Introduction

Bone tissue engineering strategies are based on combinations of cells, biomaterials and bioactive agents for tissue regeneration. Cell growth factors are considered some of the most attractive types of bioactive agents for bone tissue engineering due to their important roles in skeletal development and postnatal osteogenesis. Fibroblast growth factors (FGFs) are a group of polypeptides that control the proliferation and differentiation of various cell types [1, 2] and their important effects on the control of differentiation genes in osteoblasts have been recently recognized [3, 4]. The FGF family is presently known to include 24 closely related proteins whose expressions have been associated with bone development, growth, and repair [5, 6]. The acid fibroblast growth factor (aFGF or FGF-1) and the basic fibroblast growth factor (bFGF or FGF-2) are considered to be representative of the whole family [7, 8]. FGFs are also strong inducers of angiogenesis [9]. Neovascularization plays a pivotal role in bone development and the engineering of implantable tissues requires rapid induction of angiogenesis to meet the significant oxygen and nutrient demands of cells during tissue repair [10]. Recently, an

enhanced neovascularization has been observed in vivo with alginate microbeads loaded with FGF-1 [11].

On the other hand, silicon substituted hydroxyapatites (Si-HA) are among the most interesting bioceramics in the field of bioactive bone implants [12, 13]. Si, an essential trace element required for healthy bone and connective tissues, influences the biological activity of calcium phosphate biomaterials by modifying material properties and by direct effects on the physiological processes in skeletal tissue [14, 15]. In contact with physiological fluids, Si-HA is able to develop a new apatite phase on the surface faster than HA does. Moreover, the incorporation of Si into HA improves the bone cell proliferation and differentiation when compared to HA alone [12]. Concerning clinical practice, calcium phosphate based bioceramics are widely used as powders or granulates to fill and restore small bone defects [16]. In this sense, hydroxipatite granulates are widely used in periodontal surgery and different commercial products can be found in market. Besides, solid pieces made of sintered calcium phosphates are applied for orthopedic, cranio-maxillofacial reconstruction, otolaryngology and spinal surgery purposes, between others [17]. In the last years, there has been a growing interest in macroporous solids with 3D interconnected structures [18, 19]. These bioceramics are processed as scaffolds to improve the bone ingrowths, and are an attempt to stimulate bone regeneration instead of bone substitution. Taking all these facts into account and to provide additional biological properties for bone repair to these bioceramics, in the present study we have carried out the immobilization of FGF-1 and FGF-2 on both shapes of Si-HA biomaterials: powdered Si-HA with controlled grain size and macroporous Si-HA scaffolds prepared by rapid prototyping techniques. With these purposes, different techniques (absorbance spectroscopy, confocal microscopy, flow cytometry and scanning electron microscopy) have been used to detect the immobilization of both FGFs and to analyze the response of human Saos-2 osteoblasts to both immobilized factors through several cell parameters as morphology, size/complexity, adhesion, proliferation, cell cycle, apoptosis and reactive oxygen species content.

2 Materials and methods

2.1 Silicon substituted apatite synthesis

Silicon-substituted hydroxyapatite (Si-HA) with nominal formula $Ca_{10}(PO_4)_{5.7}(SiO_4)_{0.3}(OH)_{1.7}\square_{0.3}$, where $\square$ means vacancies at the hydroxyl position, was prepared by aqueous precipitation reaction of $Ca(NO_3)_2{\cdot}4H_2O$, $(NH_4)_2HPO_4$ and $Si(CH_3CH_2O)_4$ solutions, as described elsewhere [30]. Briefly, a 1 M solution of $Ca(NO_3)_2{\cdot}4H_2O$ was added to $(NH_4)_2HPO_4$ and $Si(CH_3CH_2O)_4$ solutions of stoichiometric concentration to obtain the composition described above. The mixture was stirred for 12 h at 80°C. The pH was kept at 9.5 by NH_3 solution addition. During the reaction the pH was continuously adjusted to 9.5 to ensure constant conditions during the synthesis. The precipitated Si-HA powder was treated at 700°C to remove nitrates without introducing important changes in the structure and microstructure of the materials [20].

Elemental chemical analysis was carried out by fluorescence X-ray spectrometry. Twelve different batches were tested to ensure the chemical homogeneity of the synthesised powders. Particle size distribution of Si-HA powder material was determined with a Sedigraph 5100 after aqueous suspension.

2.2 Preparation of rapid prototyped silicon-doped hydroxyapatite scaffolds

3D periodic macroporous scaffolds were constructed via direct write assembly of a silicon-doped hydroxiapatite slurry using a robotic deposition apparatus (envisionTEC GmbH Prefactory® 3D Bioplotter™). This technique employs a slurry delivery system mounted on a z-axis motion-controlled stage for agile printing onto a moving $x - y$ stage. The 3-axis motion is independently controlled by custom designed, computer aided direct write program (PrimCAM®). The slurry is formed by slowly addition under stirred of 29 g of silicon-doped hydroxyapatite powder over a mixture of 23 ml of monomeric aqueous solution (composed by a mixture of 35 g of methacrilamide and 5.75 g of N,N′-methylenebisacrylamide as monomers in 250 ml), 60 μg ammonium persulfate as initiator and 3.0 g Darwan 811® as surfactant. The obtained slurry is housed in a syringe (30 cm^3 disposable reservoir system Ultra™ EFD®, Nordson Company) and deposited through a conical needle (diameter = 580 μm) at the volumetric flow rate required to maintain a constant $x - y$ table speed ($v = 3$ mm/s). The final dimensions of scaffolds were 10 mm diameter ×4 mm high with interconnected pores (600 μm diameter).

The scaffolds were sterilized under UV light during 1 h and then submerged in DMEM supplemented with penicillin (800 μg/ml, BioWhittaker Europe, Belgium) and streptomycin (800 μg/ml, BioWhittaker Europe, Belgium), under a CO_2 (5%) atmosphere and at 37°C for 1 week in order to be stabilized before the cell culture.

2.3 Preparation of fibroblastic growth factors

The full-length FGF-1 (139-residues) and FGF-2 (155 residues) used in this study were synthesized and purified by Dra. R.M. Lozano (Centro de Investigaciones Biológicas, Consejo Superior de Investigaciones Cientificas,

Madrid, Spain) as described [21, 22]. FGF-1 samples were maintained as protein solution at a concentration of 1 mg/ml in 10 mM sodium phosphate (pH 7.2) containing 1.5 M NaCl at –20°C. FGF-2 samples were maintained as protein solution at a concentration of 1.4 mg/ml in 10 mM sodium phosphate (pH 7.2) containing 2 M NaCl at –20°C. For immobilization procedures, samples of soluble FGFs (200 μg of total protein) were diluted up to 6 ml with 10 mM sodium phosphate (pH 7.2) and used at a final protein concentration of 33 μg/ml in this buffer. The final concentration of NaCl was 50 mM in the samples. The final FGF solution was added to Si-HA for the immobilization assay as described below.

2.4 Immobilization of FGF-1 and FGF-2 on powdered silicon-doped hydroxyapatite

The immobilization of either FGF-1 or FGF-2 on powdered Si-HA was carried out through non-covalent binding by mixing 1 g of this biomaterial with 200 μg of soluble FGFs in 10 mM sodium phosphate (pH 7.2) in a final volume of 6 ml. The final concentration of NaCl was 50 mM in the samples. After 2 h of slight rotation at 4°C, 3 ml of the mix was lyophilized and maintained at –20°C for subsequent cell proliferation and biocompatibility assays. The rest of the mix was centrifuged 10 min at 1,000 *g* for desorption studies. The protein retention in Si-HA was calculated by absorbance spectroscopy [21, 22] through the difference of protein concentration in the supernatants before and after the protein binding to the biomaterial using as molar extinction coefficients the values of 0.79 and 0.83 for a 0.1% (1 mg/ml) solution of FGF-1 and FGF-2 respectively [22]. The scattering of the samples, measured as absorbance at 340 nm, was always subtracted in all the spectra. Absorbance spectra were recorded at 25°C in a Perkin-Elmer spectrophotometer. The amount of sample used was in the linear range of measurement of the spectrometer. Buffer (10 mM sodium phosphate and 50 mM NaCl, pH 7.2) absorbance spectrum was subtracted from all sample spectra.

2.5 Experimental desorption of FGF-1 and FGF-2 from powdered silicon-doped hydroxyapatite

The samples containing either immobilized FGF-1 or FGF-2 on powdered Si-HA were centrifuged 10 min at 1,000 × *g* and subsequently eluted using a 10 min gradient of 10 mM–1 M sodium phosphate (pH 7.2). Finally, an incubation during 10 min with 10 mM sodium phosphate (pH 7.2) containing 1.5 M NaCl was carried out. The amount of desorpted FGF after each treatment was calculated in the eluted through the protein concentration by absorbance spectroscopy [21, 22].

2.6 Immobilization of FGF-1 and FGF-2 on rapid prototyped silicon-doped hydroxyapatite scaffolds

The immobilization of either FGF-1 or FGF-2 on rapid prototyped silicon-doped hydroxyapatite scaffolds was carried out by incubation of Si-HA scaffolds with 2.5 and 10 μg/ml of each factor over night at 4°C in 1.5 ml of DMEM containing BSA 1 mg/ml. Then, the samples were frozen at –80°C for 4 h and lyophilized during 24 h at –84°C and 6×10^{-2} mB of pressure in a lyophilizer (Telstar/Lioalfa-6, Tarrasa, Spain). The presence of FGF-1 and FGF-2 on the Si-HA scaffold surface was detected by confocal laser scanning microscopy (Biorad MC1025 microscope) after immunostaining with either the primary antibody anti-FGF-1 (1:200) (polyclonal 5034-100, Bio-Vision) or the primary antibody anti-FGF-2 (1:500) (polyclonal 07-1435, Millipore) at 4°C for 2 h. DyLight 488 Donkey α-rabbit IgG (1/100) (BioLegend) was used as secondary antibody.

2.7 Cell proliferation studies

Human Saos-2 osteoblasts were seeded on 6 well culture plates (CULTEK S.L.U., Madrid, Spain, reference 153516, growth surface of 11 cm^2/well), at a density of 10^5 cells/ml (2 ml/well) in DMEM supplemented with 10% heat-inactivated fetal bovine serum (FBS, Gibco, BRL), 1 mM L-glutamine (BioWhittaker Europe, Belgium), penicillin (200 μg/ml, BioWhittaker Europe, Belgium), and streptomycin (200 μg/ml, BioWhittaker Europe, Belgium), under a CO_2 (5%) atmosphere at 37°C. To evaluate the effect on cell proliferation of either FGF-1 or FGF-2 immobilized on powered silicon-doped hydroxyapatite (Si-HA), increasing amounts of FGF-1/Si-HA and FGF-2/Si-HA were added to the culture medium (5 h after cell seeding) and the cultures were then maintained for 2 and 4 days in the presence of FGF/Si-HA. The FGF doses were 0.6, 0.8 and 1 ng/ml and the Si-HA/FGF ratio was 5 μg/1 ng. Controls either in the absence or presence of Si-HA (5 μg/ml, dose that corresponds to the highest concentration of material used in this study) but without growth factors were always carried out. After these culture times, the attached osteoblasts were washed with phosphate buffer saline (PBS) and harvested using 0.25% trypsin–EDTA solution for 15 min. The reaction was stopped with culture medium and cells were counted with a Neubauer hemocytometer for the analysis of cell proliferation. Cells were then centrifuged at 310 × *g* for 10 min and resuspended in fresh medium for the analysis of viability, cell cycle, apoptosis, reactive oxygen species (ROS) content, cell size and complexity by flow cytometry (Section 2.9).

2.8 Morphological studies by confocal microscopy

Cell morphology was studied by confocal microscopy after treatment with 1 ng/ml of either FGF-1 or FGF-2 immobilized on powered silicon-doped hydroxyapatite (5 μg) for 4 days. Controls either in the absence or presence of Si-HA (5 μg/ml, dose that corresponds to the highest concentration of material used in this study) but without growth factors were always carried out. After fixation with 3.7% paraformaldehyde in PBS for 10 min, samples were washed with PBS and permeabilizated with 0.1% Triton X-100 for 3–5 min. The samples were then washed with PBS and preincubated with PBS containing 1% BSA for 20–30 min. Then, cells were incubated for 20 min with Alexa-488 phalloidin (Dilution 1:40, Molecular Probes) which stains F-actin filaments, washed with PBS and the cell nuclei were stained with DAPI (4′-6-diamidino-2′-phenylindole, 3 μM in PBS, Molecular Probes). After staining and washing with PBS, cells were examined by a Biorad MC1025 confocal laser scanning microscope. The fluorescence of Alexa-488 was excited at 488 nm and the emitted fluorescence was measured at 510–530 nm. The fluorescence of DAPI was excited at 405 nm and measured at 420–480 nm.

2.9 Flow cytometry studies

Human Saos-2 osteoblasts were cultured 2 and 4 days either in the absence or presence of different doses of FGF-1 or FGF-2 immobilized on powered silicon-doped hydroxyapatite. The FGF doses were 0.6, 0.8 and 1 ng/ml and the Si-HA/FGF ratio was 5 μg/1 ng. Controls either in the absence or presence of Si-HA (5 μg/ml, dose that corresponds to the highest concentration of material used in this study) but without growth factors were always carried out. After culture, cells were washed twice with PBS and incubated at 37°C with trypsin–EDTA solution for cell detachment. The reaction was stopped with culture medium after 5–10 min and cells were centrifuged at 310 × *g* for 10 min and resuspended in fresh medium.

After the incubation with the different probes, as it is described below, the conditions for the data acquisition and analysis were established using negative and positive controls with the CellQuest Program of Becton–Dickinson and these conditions were maintained during all the experiments. Each experiment was carried out three times and single representative experiments are displayed. For statistical significance, at least 10,000 cells were analyzed in each sample and the mean of the fluorescences emitted by these single cells was used.

2.9.1 Cell size and complexity

The light scattering properties of cells were examined by flow cytometry in a FACScalibur Becton–Dickinson flow cytometer, measuring forward angle (FSC) and side angle (SSC) light scatters as indicators of cell size and complexity, respectively.

2.9.2 Cell cycle analysis

Cell suspensions were incubated with Hoechst 33258 (Poly-Sciences, Inc., Warrington, PA, USA) (Hoechst 5 μg/ml, ethanol 30%, and BSA 1% in PBS), used as a nucleic acid stain, for 30 min at room temperature in darkness. The fluorescence of Hoechst was excited at 350 nm and the emitted fluorescence was measured at 450 nm in a LSR Becton–Dickinson flow cytometer. The cell percentage in each cycle phase: G_0/G_1, S and G_2/M was calculated with the CellQuest Program of Becton–Dickinson and the $SubG_1$ fraction was used as indicative of apoptosis.

2.9.3 Intracellular reactive oxygen species (ROS) content

Cells were incubated at 37°C for 30 min with 100 μM 2′, 7′-dichlorofluorescein diacetate (DCFH/DA, Serva, Heidelberg/Germany). To measure the intracellular reactive oxygen species (ROS), the fluorescence of DCF (produced by DCFH oxidation) was excited by a 15 mW laser tunning to 488 nm and the emitted fluorescence was measured with a 530/30 band pass filter in a FACScalibur Becton–Dickinson flow cytometer. Cell viability was determined by addition of propidium iodide (PI; 0.005% in PBS, Sigma–Aldrich Corporation, St. Louis, MO, USA) to stain the DNA of dead cells.

2.10 Cell culture on rapid prototyped silicon-doped hydroxyapatite scaffolds

After immobilization of either FGF-1 or FGF-2 on rapid prototyped silicon-doped hydroxyapatite scaffolds, human Saos-2 osteoblasts were seeded at a density of 10^5 cells/ml in Dulbecco's Modified Eagle's Medium (DMEM, Sigma Chemical Company, St. Louis, MO, USA) supplemented with 10% fetal bovine serum (FBS, Gibco, BRL), 1 mM L-glutamine (BioWhittaker Europe, Belgium), penicillin (200 μg/ml, BioWhittaker Europe, Belgium), and streptomycin (200 μg/ml, BioWhittaker Europe, Belgium), under a CO_2 (5%) atmosphere and at 37°C for different times. The culture medium was renewed every 2 days. To evaluate the cell adhesion and proliferation on the scaffolds after different culture times, morphological studies were carried out by scanning electron microscopy (SEM). For SEM studies, the attached cells on the biomaterial were fixed with glutaraldehyde (2.5% in Phosphate Buffer Saline) for 45 min. Sample dehydration was performed by slow water replacement using series of ethanol solutions (30%, 50%, 70%, 90%) for 30 min with a final dehydration

in absolute ethanol for 60 min, allowing samples to dry at room temperature and under vacuum. Afterwards, the pieces were mounted on stubs and coated in vacuum with gold–palladium. Cells were examined with a JEOL JSM-6400 scanning electron microscope.

2.11 Statistics

Data are expressed as means ± standard deviations of a representative of three repetitive experiments carried out in triplicate. Statistical analysis was performed by using the Statistical Package for the Social Sciences (SPSS) version 11.5 software. Statistical comparisons were made by analysis of variance (ANOVA). Scheffé test was used for post hoc evaluations of differences among groups. In all statistical evaluations, $p < 0.05$ was considered as statistically significant.

3 Results and discussion

The utility of Si-doped hydroxyapatite (Si-HA) as an excellent material in the field of bone implants has been previously showed due to its biocompatibility, bioactivity and osteoconductivity [12, 13]. On the other hand, there are many studies on the exogenous administration of FGF-1 and FGF-2 into normal animals for bone fracture or bone defect healing [5, 23–25]. The problem with this kind of administration is that a large amount of FGF solution was consumed because of its rapid dispersion in vivo [26, 27]. Recent studies have been carried out for the immobilization of FGF-2 on biomaterials [28–31] and for the local delivery of bioactive molecules as promising alternative treatment for restoring bone defects [32]. To solve this problem, we have carried out the immobilization of FGF-1 and FGF-2 on both powdered Si-HA and rapid prototyped Si-HA scaffolds in order to evaluate the capacity of these systems for inducing cellular proliferation. Thus, the binding efficiency of each factor to these Si-HA biomaterials and the subsequent effects on human Saos-2 osteoblasts have been investigated with different techniques.

Figure 1a shows the particle size distribution of Si-HA powder material determined with a Sedigraph 5100 after aqueous suspension. A bimodal distribution centred at 10 and 50 microns were observed. To evaluate the binding of both FGFs to powdered silicon-doped hydroxyapatite, the concentration of both FGFs in the supernatant was evaluated by absorbance spectroscopy as is described in Section 2.4 of the materials and methods section. The obtained results in this study demonstrate that the binding of both proteins to this biomaterial was reached efficiently (95% in both cases) in our experimental conditions. To know the binding strength of either FGF-1 or FGF-2 to powdered Si-HA, different desorption assays were carried out with sodium phosphate solutions (NaP, pH 7.2) of increasing concentrations (10 mM–1 M). Table 1 shows the percentage of eluted FGF after each treatment. FGF-1 was completely desorpted after 1 M NaP treatment but, in the case of FGF-2, the addition of 1.5 M NaCl to the 10 mM NaP solution was necessary in order to obtain a 54% of elution of this immobilized factor. These data indicate that FGF-2 presents a higher binding strength to Si-HA than FGF-1.

To know if immobilized FGF-1 and FGF-2 maintain its biological activity, the proliferation human Saos-2 osteoblasts was evaluated in the presence of different concentrations of each factor immobilized on powdered Si-HA. Previously, the effect of this biomaterial (5 μg/ml of Si-HA) without FGFs was analyzed on this cell type.

Saos-2 is a human osteosarcoma cell line with osteoblastic properties as production of mineralized matrix, high levels of alkaline phosphatase, PTH receptors coupled to adenylate cyclase and osteonectin presence [33]. Due to these properties, this cell line is usually used as experimental model in this kind of in vitro studies [34, 35]. The Saos-2 cells used in all experiments were below passage 20 in order to ensure the phenotypic stability of these cells [36]. Cell adhesion and proliferation processes are good indicators of the response that could be expected when a

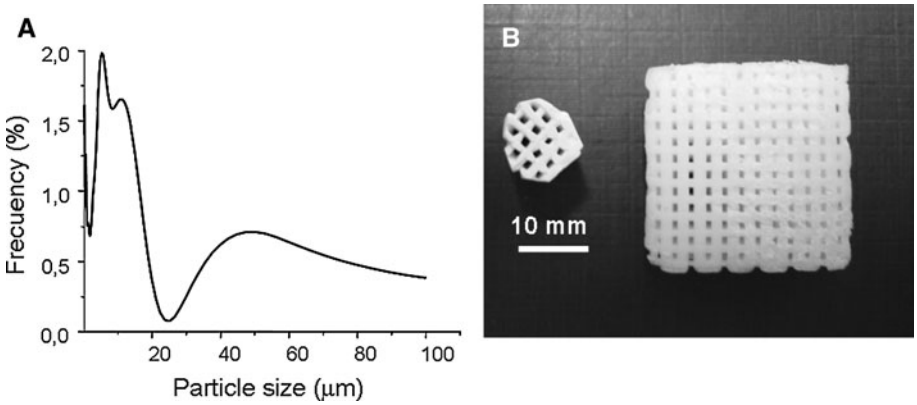

Fig. 1 **a** Particle size distribution of Si-HA powder material, determined with a Sedigraph 5100 after aqueous suspension. A bimodal distribution centred at 10 and 50 microns are observed. **b** Si-HA scaffolds prepared with a rapid prototyping 3D printing Bioplotter equipment

Table 1 Elution of bound FGF from powered Si-HA

Treatment	Eluted FGF-1 (%)	Eluted FGF-2 (%)
NaP 10 mM (T0)	0	0
NaP 100 mM (T1)	0	0
NaP 400 mM (T2)	65	11
NaP 1 M (T3)	35	20
NaP 10 mM+1.5 M NaCI (T4)	0	23

biomaterial is used in vivo. Osteoblasts rapidly adhered, spread and proliferated in the presence of powdered Si-HA (5 μg/ml), dose that corresponds to the highest concentration of material used in this study, and the cell density was maintained at level corresponding to that for the control after 2 days culture (Fig. 2a). After 4 days culture, osteoblasts continued proliferating in the presence of Si-HA but the cell number was below control (Fig. 2b). In this sense, we have recently reported that osteoblasts showed a higher sensitivity than other cell types to hydroxyapatite-βTCP/agarose biomaterial [37, 38].

To evaluate the bioactivity of immobilized FGF-1 and FGF-2 on powdered Si-HA, the proliferation of Saos-2 osteoblasts in the presence of different doses of Si-HA/FGF-1 and Si-HA/FGF-2 was evaluated after 2 and 4 days culture.

As it can be observed in Fig. 2, both immobilized FGFs produced a gradual increase of osteoblast proliferation after 2 and 4 days culture in a time and dose dependent manner. At short culture times (2 days), a stimulation of osteoblast proliferation was observed at all dose levels of both factors except at 1 ng/ml of FGF-1 (Fig. 2a). After 4 days culture (Fig. 2b), the presence of immobilized FGF-1 and FGF-2 continued stimulating the growth of this cell type at all dose levels except at 1 ng/ml of FGF-2. These findings are in agreement with the belt-shaped for FGF-2 response curves described by U. Mayr-Wohlfart et al. [39]. However, our results are somewhat different from those of Lind et al. [40] who found maximal stimulation of human trabecular osteoblasts from the iliac crest by FGF-2 at 100 ng/ml.

On the other hand, it has been recently shown that 1 ng/ml of FGF-1 induces an angiogenic response with a more morphologically normal and more durable neovascular network versus higher FGF-1 concentration (10–100 ng/ml) [41]. The effective concentrations of FGF-2 for various biological reactions were determined in many previous studies [23, 27]. These previous studies suggest that FGF-2 at concentration higher than 10 μg/ml may have adverse effects on bone formation. Recently, Sogo et al. showed a maximum of 2.72 μg/cm^2 of FGF-2 immobilized on the HAP ceramic with ability to promote new bone formation [25]. The clinical use of very high concentrations of growth

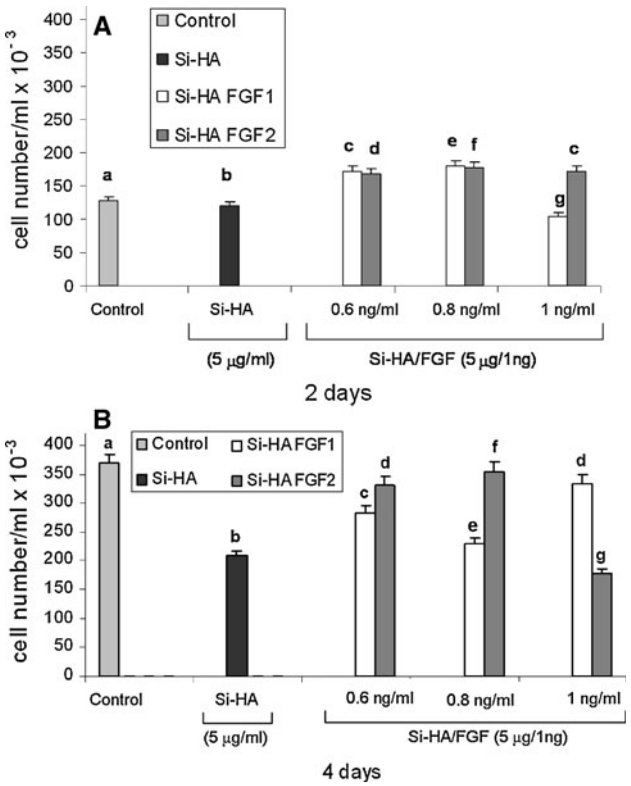

Fig. 2 **a** Proliferation of Saos-2 osteoblasts after 2 days in the presence of FGF-1 and FGF-2 immobilized on powered silicon-doped hydroxyapatite. The FGF doses were 0.6, 0.8 and 1 ng/ml and the Si-HA/FGF ratio was 5 μg/1 ng. Osteoblast cultures either in the absence (control) or presence of Si-HA (5 μg/ml, dose that corresponds to the highest concentration of material used in this study) without growth factors were also carried out. Columns with the same letter at the top are statistically equivalent (without significant differences). Columns with different letters (*a–g*) at the top are statistically different. Statistical significance: ***$P < 0.005$. **b** Proliferation of Saos-2 osteoblasts after 4 days in the presence of FGF-1 and FGF-2 immobilized on powered silicon-doped hydroxyapatite. The FGF doses were 0.6, 0.8 and 1 ng/ml and the Si-HA/FGF ratio was 5 μg/1 ng. Osteoblast cultures either in the absence (control) or presence of Si-HA (5 μg/ml, dose that corresponds to the highest concentration of material used in this study) without growth factors were also carried out. Columns with the same letter at the top are statistically equivalent (without significant differences). Columns with different letters (*a–g*) at the top are statistically different. Statistical significance: ***$P < 0.005$

factor may be accompanied by unwanted side effects, such as stimulation of tumor growth, abnormal vascular function, hypotension, and hypervascularity [41].

The present study indicate the maintenance of the biological activity of both FGF-1 and FGF-2 factors after its immobilization on powdered Si-HA and demonstrate the sensitivity and response capacity of osteoblasts to these systems.

In order to study the morphology of osteoblasts cultured in the presence of FGF-1 and FGF-2 immobilized on powdered silicon-doped hydroxyapatite and to know if this

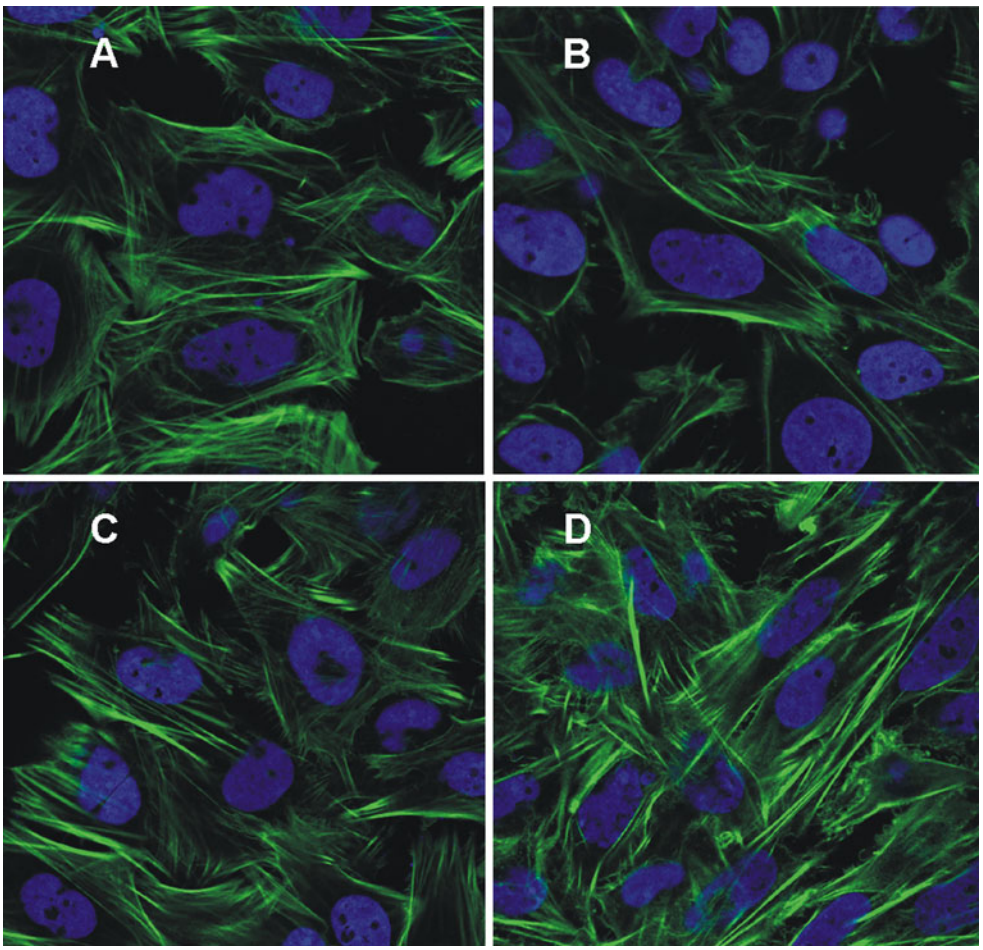

Fig. 3 Morphology evaluation by confocal microscopy of Saos-2 osteoblasts cultured in the presence of FGF-1 and FGF-2 immobilized on powered silicon-doped hydroxyapatite. Osteoblasts were cultured for 4 days in the presence of either Si-HA/FGF-1 (C, 1 ng FGF-1/ml) or Si-HA/FGF-2 (D, 1 ng FGF-2/ml). Osteoblast cultures either in the absence (**a**) or presence of Si-HA (5 μg/ml, dose that corresponds to the highest concentration of material used in this study) without growth factors (**b**), were also carried out. Cells were stained with DAPI (for the visualization of the cell nuclei) and Alexa-488 phalloidin (for the visualization of cytoplasmic F-actin filaments)

biomaterial (with or without each factor) induces apoptosis, fluorescence studies were carried out by confocal microscopy. The images of Fig. 3 show osteoblasts well spread in the presence of the Si-HA, Si-HA/FGF-1 and Si-HA/FGF-2 biomaterials after staining with Alexa-488 phalloidin and DAPI. Cells presented their correct morphology with a distinctive actin network and no apoptotic bodies in nuclei were detected thus indicating the absence of apoptosis in all cases.

Since cell-biomaterial interactions can modify the cell size and complexity [42], these parameters were evaluated by flow cytometry analyzing the FSC (forward angle light scatter) and SSC (90° side angle light scatter) of Saos-2 osteoblasts cultured for 2 and 4 days in the presence of different doses of powdered Si-HA/FGF-1 and Si-HA/FGF-2. Figure 4 shows the light-scattering properties of Saos-2 osteoblasts after 4 days culture either in the absence (Fig. 4a) or presence of Si-HA/FGF-1 (1 ng FGF-1/ml, Fig. 4c) and Si-HA/FGF-2 (1 ng FGF-2/ml, Fig. 4d). Controls with this biomaterial without growth factors were also carried out (Fig. 4b). No significant differences were obtained. These results indicate that the interaction with powdered Si-HA/FGF biomaterials did not produce changes of volume, density or cytoplasmic granularity on osteoblasts and confirm the correct size and complexity of this cell type. On the other hand, the cell cycle of Saos-2 osteoblasts cultured in the presence of different doses of Si-HA/FGF-1 and Si-HA/FGF-2 was studied by flow cytometry after 2 and 4 days culture. Figure 5 shows the G_0/G_1, S and G_2/M cycle phases of Saos-2 osteoblast after 4 days culture either in the absence (Fig. 5a) or presence of Si-HA/FGF-1 (1 ng FGF-1/ml, Fig. 5c) and Si-HA/FGF-2 (1 ng FGF-2/ml, Fig. 5d). Controls with this biomaterial without growth factors were also carried out (Fig. 5b). No significant differences were obtained when analyzing the cell percentage in each cycle phase after these treatments.

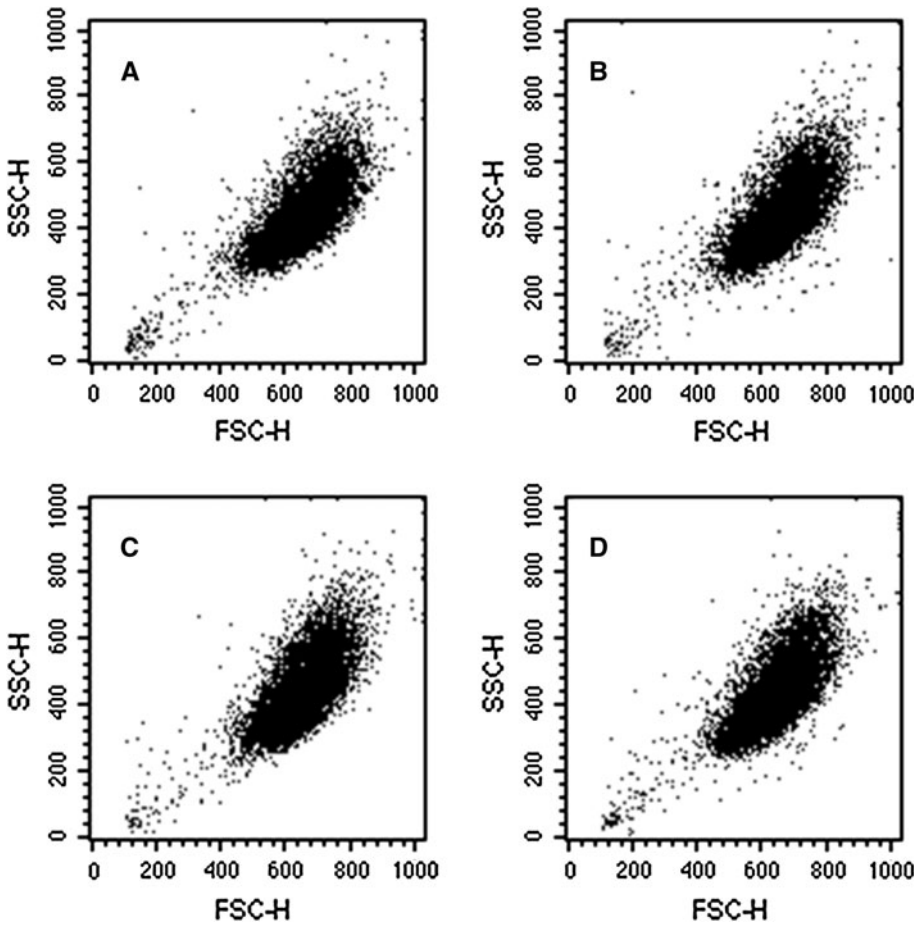

Fig. 4 Light-scattering properties of Saos-2 osteoblasts cultured in the presence of FGF-1 and FGF-2 immobilized on powered silicon-doped hydroxyapatite. Osteoblasts were cultured for 4 days in the presence of either Si-HA/FGF-1 (C, 1 ng FGF-1/ml) or Si-HA/FGF-2 (D, 1 ng FGF-2/ml). Osteoblasts cultures either in the absence (**a**) or presence of Si-HA (5 μg/ml, dose that corresponds to the highest concentration of material used in this study) without growth factors (**b**) were also carried out. Forward angle (FCS) and 90° side angle (SSC) light scatters were analyzed by flow cytometry as a measurement of cell size and internal complexity, respectively. Figure shows a representative of three repetitive experiments. In each sample, 10,000 cells were analyzed

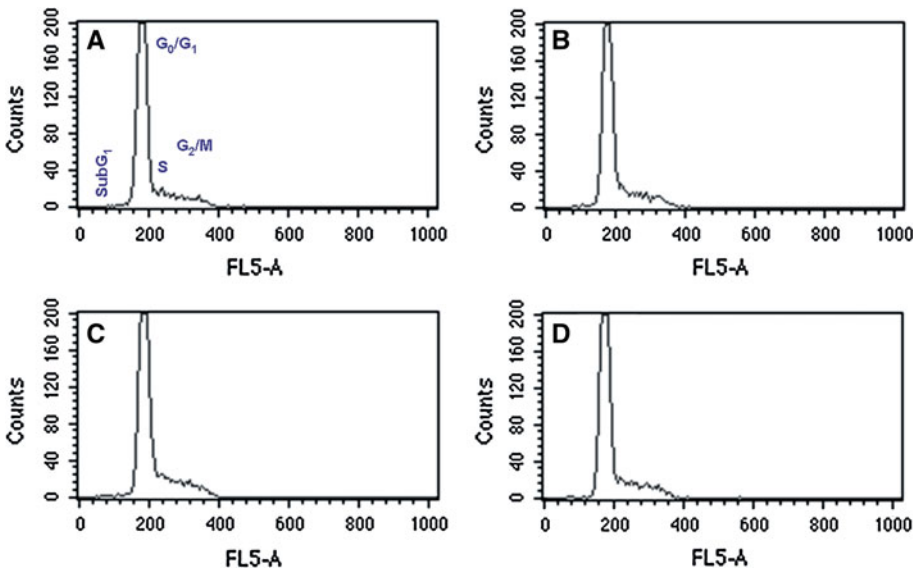

Fig. 5 Cell cycle analysis of Saos-2 osteoblasts cultured in the presence of FGF-1 and FGF-2 immobilized on powered silicon-doped hydroxyapatite. Osteoblasts were cultured for 4 days in the presence of either Si-HA/FGF-1 (C, 1 ng FGF-1/ml) or Si-HA/FGF-2 (D, 1 ng FGF-2/ml). Osteoblast cultures either in the absence (**a**) or presence of Si-HA (5 μg/ml, dose that corresponds to the highest concentration of material used in this study) without growth factors (**b**) were also carried out. Figure shows the G_0/G_1, S and G_2/M cycle phases of a representative of three repetitive experiments. $SubG_1$ fraction was used as indicative of apoptosis. In each sample, 10,000 cells were analyzed

Since $SubG_1$ fraction is attributed to cells with fragmented DNA, it was used as indicative of apoptosis. The analysis of $SubG_1$ fraction showed the absence of apoptosis, in agreement with the confocal microscopy studies (Fig. 3). To measure the intracellular reactive oxygen species content (ROS) in Saos-2 osteoblasts cultured in the presence of powdered biomaterials Si-HA, cells were detached by trypsinization and incubated with the DCFH/DA probe which can cross the plasma membrane. Inside the cell, DCFH (non fluorescent) is released from DCFH/DA by cytosolic esterases, and the oxidation of DCFH to DCF (fluorescent) produces high fluorescence intensities in cells. The emitted fluorescence of DCF at 530 nm was determined by flow cytometry as a measure of intracellular reactive oxygen species. This parameter did not show significant differences between control cells and cells cultured in the presence of powdered Si-Ha with or without immobilized growth factors (data no shown). The obtained results indicate the non existence of oxidative stress induced by the powdered Si-HA/FGF biomaterials in Saos-2 osteoblasts.

Highly porous scaffolds are generally designed as the substrate for anchorage dependent cells and to facilitate nutrient and metabolite distribution necessary for cell growth and new bone tissue formation [43, 44]. Thus, once carried out the immobilization and bioactivity evaluation of FGF-1 and FGF-2 on powdered Si-HA, we have carried out the immobilization of FGF-1 and FGF-2 on rapid prototyped silicon-doped hydroxyapatite scaffolds (Fig. 1b). With this purpose, Si-HA disks of 10 mm diameter ×4 mm high with interconnected pores (600 μm diameter) were incubated with 2.5 and 10 μg/ml of FGF-1 and FGF-2 (as described in Materials and Methods, Section 2.6) and the presence of each factor on the scaffold surface was detected by confocal microscopy after immunostaining with specific antibodies. Figure 6a–d represents the projection of the images captured along the z axis every 70 μm with the confocal microscope in each case. As it can be observed, both FGF-1 and FGF-2 were widely detected on the surface of Si-HA scaffolds. Controls without FGF treatment and subsequent treatment of the secondary antibody showed the absence of fluorescence obtaining black images (data not shown). These results indicate the specificity of the FGF immobilization on these scaffolds.

The capacity to keep osteoblast adhesion and proliferation of rapid prototyped Si-HA scaffolds after FGF-1 and FGF-2 immobilization was also evaluated in the present study as fundamental requisite for a biomaterial designed

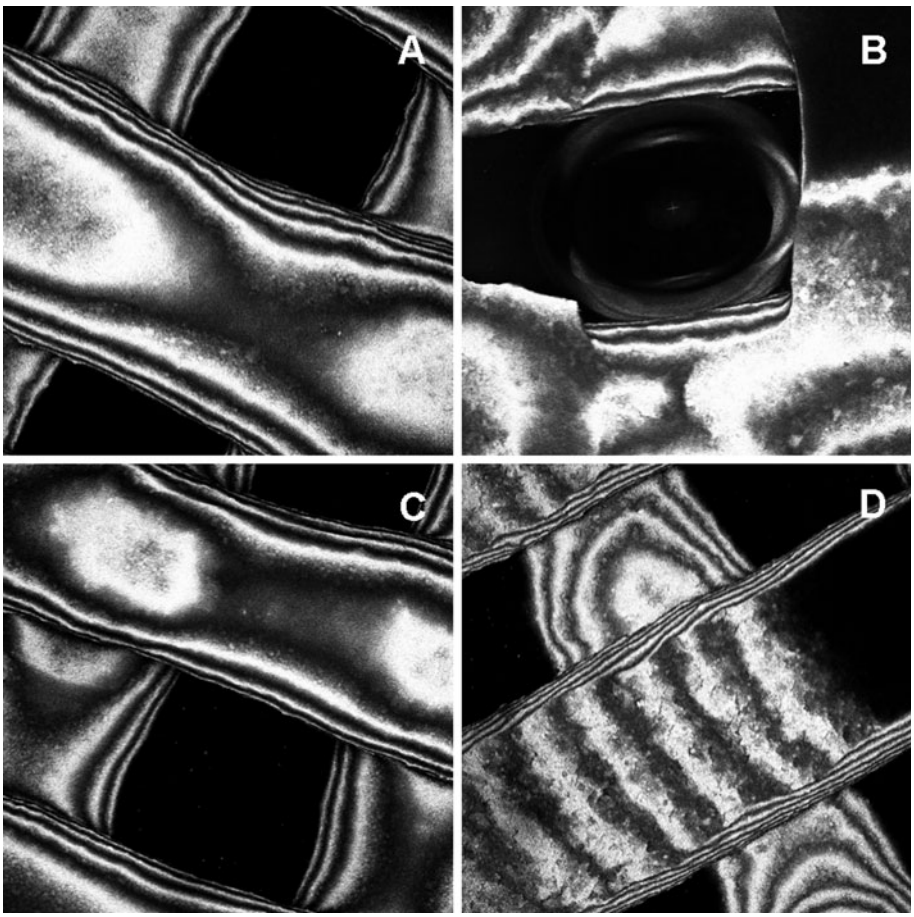

Fig. 6 Detection of FGF-1 and FGF-2 fibroblastic growth factors immobilized on rapid prototyped silicon-doped hydroxyapatite scaffolds by confocal laser scanning microscopy. **a** and **b** FGF-1 detection on the scaffold surface after incubation treatment with 2.5 μg/ml and 10 μg/ml of this growth factor, respectively. **c** and **d** FGF-2 detection on the scaffold surface after incubation treatment with 2.5 μg/ml and 10 μg/ml of this growth factor, respectively. The figures represent the projection of the images captured along the z axis every 70 μm with the confocal microscope in each case. Control without FGF treatment and subsequent treatment of the secondary antibody were showed the absences of fluorescence (data not show)

for bone substitution and repair. Thus, to know the osteoblast behaviour in contact with FGF/Si-HA scaffolds, the cell morphology was analyzed by scanning electron microscopy (SEM) after 4 days culture on rapid prototyped silicon-doped hydroxyapatite scaffolds with immobilized FGF-1 and FGF-2 at different concentrations. Figure 7a shows the appearance of the macroporous Si-HA scaffolds with a regular surface. In Fig. 7b individual cells on the surface of these scaffolds without FGFs can be observed. Figure 7c, d shows osteoblasts grown on macroporous Si-HA samples after immobilization of FGF-1 (2.5 and 10 μg/ml respectively). Figure 7e, f corresponds to osteoblasts cultured on Si-HA scaffolds after immobilization of FGF-2 (2.5 and 10 μg/ml respectively). As it can be

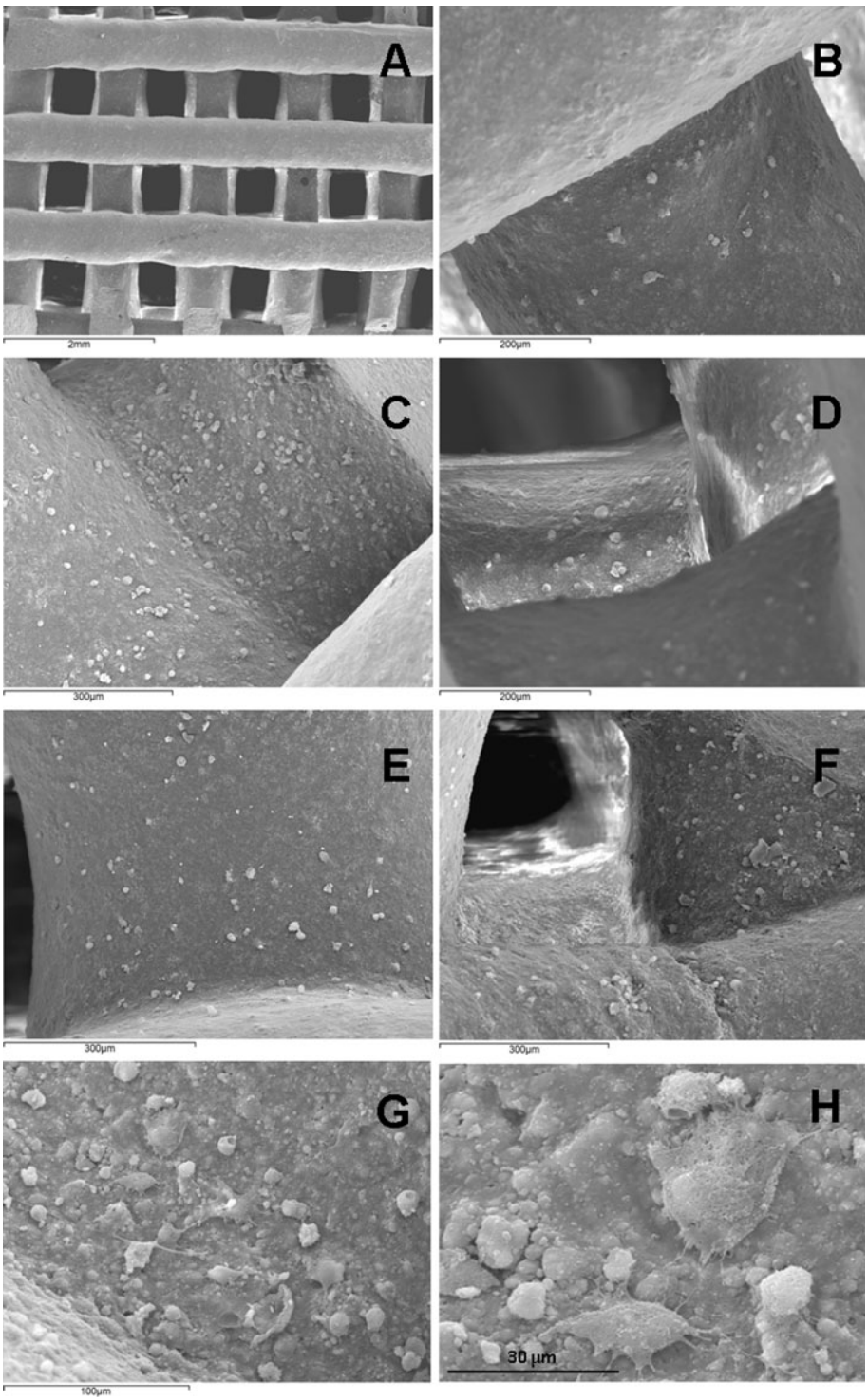

Fig. 7 Morphology evaluation by scanning electron microscopy of Saos-2 osteoblasts cultured on rapid prototyped silicon-doped hydroxyapatite scaffolds after FGF-1 and FGF-2 immobilization. Saos-2 osteoblasts were cultured for 4 days on: **a** and **b** rapid prototyped silicon-doped hydroxyapatite scaffolds without growth factors; **c** and **d** scaffolds with 2.5 μg/ml and 10 μg/ml of FGF-1 previously immobilized, respectively; **e** and **f** scaffolds with 2.5 μg/ml and 10 μg/ml of FGF-2 previously immobilized, respectively. **g** and **h** Magnifications of scaffolds with immobilized FGF-1 (2.5 μg/ml) allow to observe better the osteoblast morphology

observed in all cases, Saos-2 osteoblasts adhered to the scaffolds with immobilized FGFs, proliferated and colonized its surface. This interaction did not alter the osteoblast morphology, showing typical bone cell characteristics: cube-shape, less elongated than fibroblasts and big sized (Fig. 7g, h). It was appreciable that in some areas, biomaterial surface was extensively covered by osteoblasts. These areas correspond to cells growth on silicon-doped hydroxyapatite scaffold after treatment with 2.5 μg/ml of FGF-1 (Fig. 7c) and 10 μg/ml of FGF-2 (Fig. 7f). Taking into account the observed cell proliferation onto developed material, it can be assumed that many cells penetrated the material and developed a good contact that allowed to the cells firstly adhere, spread and finally proliferate adequately. In order to quantify the promotion of cell proliferation by immobilized FGFs on 3D scaffolds, the cell number observed in different SEM images (taking the scaffold area surface into account) has been counted. The analysis of SEM images revealed that FGF immobilization on 3D scaffolds produced 50–75% increase of osteoblast proliferation. Thus, we can conclude that the immobilization of FGF-1 and FGF-2 on silicon-doped hydroxyapatite scaffolds promotes the osteoblast-scaffold adhesion and improves the proliferation capacity of this cell type.

4 Conclusions

Powdered Si-HA and rapid prototyped Si-HA scaffolds are suitable biomaterials for FGF-1 and FGF-2 immobilization. FGF-1 and FGF-2 maintain its biological activity on human osteoblasts after its immobilization on powdered Si-HA and both growth factors improve the osteoblast adhesion and proliferation onto Si-HA scaffolds suggesting the potential utility of these FGF/scaffolds for bone tissue engineering.

Acknowledgments This study was supported by research grants from Comunidad de Madrid (S-0505/MAT/0324 and S2009/MAT-1472) and Ministerio Ciencia e Innovación (MAT2008-06719-C03-02). M. Alcaide and C. Ramírez-Santillán are greatly indebt to the Universidad Complutense de Madrid for a fellowship. The authors wish to thank also to the staff of the Microscopy and Cytometry Center of the Universidad Complutense de Madrid (Spain) for the assistance in the scanning electron microscopy, flow cytometry and confocal microscopy studies.

References

1. Jaye M, Schlessinger J, Dionne CA. Fibroblast growth factor receptor kinases: molecular analysis and signal transduction. Biochim Biophys Acta. 1992;1135:185–99.
2. Basilico C, Moscatelli D. The FGF family of growth factors and oncogenes. Adv Cancer Res. 1992;59:115–65.
3. Marie PJ. Fibroblast growth factor signaling controlling osteoblast differentiation. Gene. 2003;316:23–32.
4. Marie PJ, Debiais F, Hay E. Regulation of human cranial osteoblasts phenotype by FGF-2, FGFR-2 and BMP-2 signaling. Cell Mol Biol. 2002;17:877–85.
5. Kelpke SS, Zinn R, Rue LW, Thompson JA. Site-specific delivery of acidic fibroblast growth factor stimulates angiogenic and osteogenic responses in vivo. J Biomed Mater Res. 2004; 71A:316–25.
6. Ornitz DM, Marie PJ. FGF signaling pathways in endochondral and intramembranous bone development and human genetic disease. Genes Dev. 2002;16:1446–65.
7. Nishimura T, Utsunomiya Y, Hoshikawa M, Ohuchi H, Itoh N. Structure expression of a novel human FGF, FGF-19, expressed in the fetal brain. Biochim Biophys Acta. 1999;1444:148–51.
8. Coulier F, Pontarotti P, Roubin R, Hartung H, Goldfarb M, Birnbaum DJ. Of worms and men: an evolutionary perspective on the fibroblast growth factor (FGF) and FGF receptor families. Mol Evol. 1997;44:43–56.
9. Jonca F, Ortega N, Gleizes P, Bertrand PlouetJ. Cell release of bioactive fibroblast growth factor 2 by exon 6-encoded sequence of vascular endothelial growth factor. J Biol Chem. 1997;272: 24203–9.
10. Wieghaus KA, Capitosti SM, Anderson CR, Price RJ, Blackman BR, Brown ML, Botchway EA. Small molecule inducers of angiogenesis for tissue engineering. Tissue Eng. 2006;12: 1903–13.
11. Moya ML, Garfinkel MR, Liu X, Lucas S, Opara EC, Greisler H, Brey EM. Fibroblast growth factor-1 (FGF-1) loaded microbeads enhance local capillary neovascularization. J Surg Res. 2009;160: 208–12.
12. Vallet-Regí M, Arcos D. Silicon substituted hydroxyapatites. A method to upgrade calcium phosphate based implants. J Mater Chem. 2005;15:1509–16.
13. Arcos D, Sánchez-Salcedo S, Izquierdo-Barba I, Ruiz L, González Calbet J, Vallet-Regí M. Crystallochemistry, textural properties, and in vitro biocompatibility of different silicon-doped calcium phosphates. Biomed Mater Res. 2006;78:762–71.
14. Pietak AM, Reid JW, Stott MJ, Sayer M. Silicon substitution in the calcium phosphate bioceramics. Biomaterials. 2007;28: 4023–32.
15. Thian ES, Huang J, Best SM, Barber ZH, Brooks RA, Rushton N, Bonfield W. The response of osteoblasts to nanocrystalline silicon-substituted hydroxyapatite thin films. Biomaterials. 2006;27: 2692–8.
16. Vallet-Regí M. Ceramics for medical applications. J Chem Soc Dalton Trans. 2001;2:97–108.
17. Dorozhkin SV. Bioceramics of calcium orthophosphates. Biomaterials. 2010;31:1465–85.
18. Yang A, Leong KF, Du Z, Chua CK. The design of scaffolds for use in tissue engineering. Part II. Rapid prototyping techniques. Tissue Eng. 2002;8:1–11.
19. Hollister SJ. Porous scaffold design for tissue engineering. Nat Mater. 2005;4:518–24.
20. Arcos D, Rodríguez-Carvaja J, Vallet-Regí M. Silicon incorporation in hydroxylapatite obtained by controlled crystallization. Chem Mater. 2004;16:2300–8.
21. Cuevas P, Carceller F, Lozano RM, Zazo M, Giménez-Gallego G. Protection of rat myocardium by mitogenic and non-mitogenic fibroblast growth factor during post-ischemic reperfusion. Growth Factors. 1997;15:29–40.
22. Zazo M, Lozano RM, Ortega S, Varela J, Díaz-Orejas R, Ramírez JM, Giménez-Gallego G. High-level synthesis in *Escherichia coli* of shortened and full-length human acidic fibroblast growth factor and purification in a form stable in aqueous solutions. Gene. 1992;113:231–8.

23. Nakamura T, Hanada K, Tamura M, Shibanushi T, Nigi H, Tagawa M, Fukumoto S, Matsumoto T. Stimulation of endosteal bone formation by systemic injections of recombinant basic fibroblast growth factor in rats. Endocrinology. 1995;136: 1276–84.
24. Tang KT, Capparelli C, Stein JL, Stein GS, Lian JB, Huber AC. Acidic fibroblast growth factor inhibits osteoblast differentiation in vitro: altered expression of collagenase, cell growth-related and mineralization-associated genes. J Cell Biochem. 1996;61: 152–66.
25. Sogo Y, Ito A, Onoguchi M, Oyane A, Tsurushima H, Ichinose N. Formation of a FGF-2 and calcium phosphate composite layer on hydroxyapatite ceramic for promoting bone formation. Biomed Mater. 2007;2:175–80.
26. Nakamura T, Hara Y, Tagawa M, Tamura, Yuge T, Fukuda H, Nigi H. Recombinant human basic fibroblast growth factor accelerates fracture healing by enhancing callus remodeling in experimental dog tibial fracture. J Bone Miner Res. 1998;13: 942–9.
27. Selvig KA, Wikesjo UM, Bolge GC, Finkelman RD. Impaired early bone formation in periodontal fenestration defects in dogs following application of insulin-like growth factor: II. Basic fibroblast growth factor and transforming growth factor b1. J Clin Periodontol. 1994;21:380–5.
28. Campbell PG, Miller ED, Fisher GW, Walker LM, Weiss LE. Engineered spatial patterns of FGF-2 immobilized on fibrin direct cell organization. Biomaterials. 2005;6:6762–70.
29. Shen H, Hu X, Bei J, Wang S. The immobilization of basic fibroblast growth factor on plasma-treated poly(lactide-co-glycolide). Biomaterials. 2008;29:2388–99.
30. Layman H, Spiga MG, Brooks T, Pham S, Webster KA, Andreopoulos FM. The effect of the controlled release of basic fibroblast growth factor from ionic gelatine-based hydrogels on angiogenesis in a murine critical limb ischemic model. Biomaterials. 2007;28:2646–54.
31. Lee SH, Shin H. Matrices and scaffolds for delivery of bioactive molecules in bone and cartilage tissue engineering. Adv Drug Deliv Rev. 2007;59:339–59.
32. Mabilleau G, Aguado E, Stancu IC, Cincu C, Baslé MF, Chappard D. Effects of FGF-2 release from a hydrogel polymer on bone mass and michroarchitecture. Biomaterials. 2008;29:1593–600.
33. Rodan SA, Imai Y, Thiede MA, Wesolowski G, Thompson D, Bar-Shavit Z, Shull S, Mann K, Rodan GA. Characterization of a human osteosarcoma cell line (Saos-2) with osteoblastic properties. Cancer Res. 1987;47:4961–6.
34. Fassina L, Visai L, Asti L, Benazzo F, Speziale P, Tanzi MG, Mageneset G. Calcified matrix production by SAOS-2 cells inside a polyurethane porous scaffold, using a perfusion bioreactor. Tissue Eng. 2005;11:685–700.
35. Mayr-Wohlfart U, Fiedler J, Günther KP, Puhl W, Kessler S. Proliferation and differentiation rates of a human osteoblast-like cell line (Saos-2) in contact with different bone substitute materials. J Biomed Mater Res. 2001;57:132–9.
36. Hausser HJ, Brenner RE. Phenotypic instability of Saos-2 cells in long-term culture. Biochem Biophys Res Commun. 2005;333: 216–22.
37. Alcaide M, Serrano MC, Pagani R, Sánchez-Salcedo S, Nieto A, Vallet-Regí M, Portolés MT. Biocompatibility markers for the study of interactions between osteoblasts and composite biomaterials. Biomaterials. 2009;30:45–51.
38. Alcaide M, Serrano MC, Pagani R, Sánchez-Salcedo S, Nieto A, Vallet-Regí M, Portolés MT. L929 fibroblast and SAOS-2 osteoblast response to hydroxyapatite-βTCP/agarose biomaterial. J Biomed Mater Res. 2009;89:539–54.
39. Mayr-Wohlfart U, Waltenberger J, Hausser H, Kessler S, Günther KP, Dehio C, Puhl W, Brenner RE. Vascular endothelial growth factor stimulates chemotactic migration of primary human osteoblasts. Bone. 2002;30:472–7.
40. Lind M, Deleuran B, Thestrup-Pedersen K, Soballe K, Eriksen EF, Bunger C. Chemotaxis of human osteoblasts. Effects of osteotropic growth factors. APMIS. 1995;103:140–6.
41. Brey EM, Uriel S, Greisler HP, McIntire LV. Therapeutic neovascularisation: contribution from bioengineering. Tissue Eng. 2005;11:567–84.
42. Serrano MC, Pagani R, Peña J, Portolés MT. Transitory oxidative stress in L929 fibroblasts cultured on poly (ε-caprolactone) films. Biomaterials. 2005;26:5827–34.
43. Ma PX, Zhang R, Xiao G, Francheschi R. Engineering new bone tissue in vitro on highly porous poly(α-hydroxyacids)/hydroxyapatite composite scaffolds. J Biomed Mater Res. 2001;54: 284–93.
44. Kim HJ, Kim UJ, Kim HS, Li C, Wada M, Leisk GG, Kaplan DL. Bone tissue engineering with premineralized silk scaffolds. Bone. 2008;42:1226–34.